論 文 の 内 容 の 要 旨

論文題目 Transport and NMR studies of an organic crystal α-$(BEDT-TTF)_2I_3$ in the critical region of charge order-to-Dirac fermion transition

（電荷秩序-ディラックフェルミオン転移の臨界領域にある
有機結晶 α-$(BEDT-TTF)_2I_3$ の電荷輸送および NMR 研究）

氏　　名　　劉　東

1. Introduction

This thesis explores the critical region of a charge order (CO)-to-Dirac Fermion (DF) transition in the quasi-two-dimensional layered organic conductor α-$(BEDT-TTF)_2I_3$ (abbreviated as α-I_3 hereafter) (Fig. 1(a, b)). The study has been motivated by the proximity of a strongly correlated CO state [1] and a massless DF state [2,3] right beside each other in the phase diagram in α-I_3 (Fig. 2(a)), which affords us an unprecedented opportunity to investigate the interplay between the correlation and the massless nature of electrons. Besides, the unique features of massless DFs in α-I_3 distinguished from other DF systems have also been our motivation as listed in the following. First, the electron interaction strength could be tuned continuously by applying pressure, and an evolutionary growing up of the strong correlation effects are expected on approaching the CO-DF phase boundary until finally, mass acquisition in the CO state. Second, massive works based on the well-known DF system in graphene have been elucidating the interacting DFs mainly by investigating the charge degrees of freedom; for the bulk crystal α-I_3, however, it is expected to uncover both of the spin and charge behaviors by electron transport and nuclear magnetic resonance (NMR) measurements under pressures. Third, the tilted nature of the Dirac cone in α-I_3 (Fig. 1(c)) further enriches the correlation effects of DFs. Forth, the Dirac point in α-I_3 could be closely approached in a super-clean condition while the low-energy charge carriers' distribution characterized by electron and hole puddles are indicated in graphene [4].

In the thesis, we describe our experimental investigation of the CO and DF states in α-I_3 under pressure variation. An introduction to the background on massless Dirac fermions and α-I_3 is given in

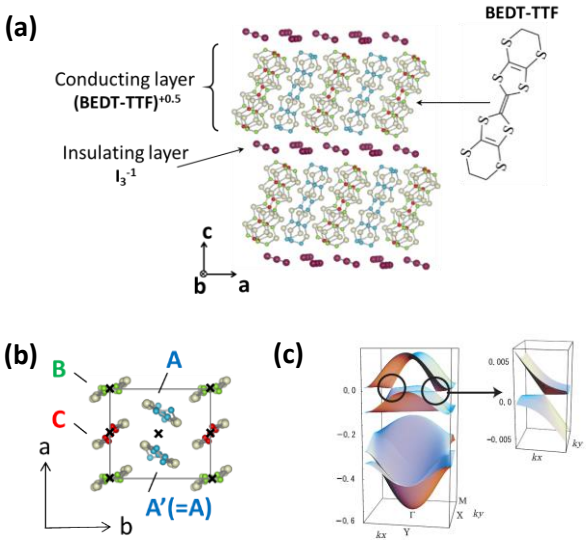

Fig. 1 Crystal structure of α-I_3 looking from (a) b-axis and (b) c-axis. (c) Tilted Dirac cone in α-I_3 under pressure [3].

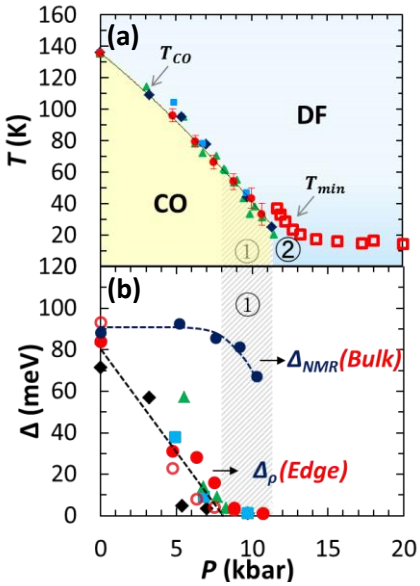

Fig. 2 (a) P-T phase diagram. (b) Pressure dependent charge(Δ_ρ) and spin(Δ_{NMR}) excitation gap.

Sec.1. The experimental details are described in Sec. 2. Sec.3 is devoted to the results and discussions. First of all (Sec. 3.1), a pressure-temperature (*P*-*T*) diagram is established based on the charge and spin behaviors probed by electrical resistance and ^{13}C NMR. We found that the CO and spin singlet transitions occur almost at the same time and is gradually suppressed by pressure until suddenly disappearing at the critical pressure of P_c= 11 kbar, above which the DF phase is stabilized as a ground state. Sec. 3.2 presents the results and discussions for the CO state in which the emergence of edge states is implied. In Sec. 3.3, we present the results and discussions for the DF state. We demonstrated two contrary renormalization behaviors in the high and low temperature regimes. The DF state in the vicinity of the critical pressure P_c is revealed to be distinctive from the state far away from the boundary in both the charge and spin degrees of freedoms.

2. Experimental

Single crystals of α-I_3 are synthesized by the conventional electrochemical oxidization method. The typical size of the crystals is 1 mm (along a axis) × 0.3 mm (along b axis) in the conducting plane, and 10 to 100 μm in thickness (along c axis) (Fig. 1(a, b)). The electrical resistivity measurements are performed with a current flowing along a axis by the four-terminal method. Electrodes were made by attaching gold wires of 25 μm in diameter along a axis on a sample surface with carbon paste.

For NMR measurements, the central carbon sites in BEDT-TTF molecules are selectively enriched by ^{13}C isotopes (nuclear spin I = 1/2) with 99% concentration (Fig. 1(a)). NMR spectra are obtained by the Fourier transformation of spin-echo signals. Spin-lattice relaxation rate T_1^{-1} is determined by the saturation and recovery method. A magnetic field of 6T generated by a superconducting split-pair magnet is applied parallel to the a-b conducting plane in ^{13}C NMR experiments.

A crystal is put in a Teflon capsule filled with the oil Daphne 7373 as a pressure-transmitting medium

and then the capsule is mounted in a clamp-type pressure cell with which hydrostatic pressures are applied. All the pressure values given are the pressures applied at room temperature before cooling.

3. Results and Discussions

3.1 Determination of the *P-T* phase diagram

We first established the *P-T* phase diagram by the transport and NMR results (Fig. 2 (a)). The critical pressure (P_c) for the CO-to-DF ground-state transition was confirmed to be approximately 11 kbar by a drastic change in the temperature-dependent behavior of charge transport and (static and dynamic) spin susceptibility. For $P< P_c$, the first-order transition line (T_{co}) separating the DF and the CO state in the *P-T* phase diagram was identified with the metal-insulator transition in electrical resistivity (ρ) under pressures. For $P> P_c$, a remarkable growth of the low-temperature resistivity upturn (Fig. 3(c)) is observed in the vicinity of P_c and the temperature at which resistivity reaches a minimum, T_{min}, is located in the phase diagram. The upturn is found to be enhanced in a near-critical manner below 15 kbar.

3.2 CO state (P<11 kbar, $T<T_{co}$)

The CO state was characterized by four parameters in the present experiments: (1) Charge-ordering temperature (T_{co}) identified by a steep increase in ρ on cooling (Fig. 2(a)), which is continuously suppressed by pressure until discontinuously dropping to 0 K at P_c; (2) Spin-singlet transition temperature (T_{ss}) where the paramagnetic shift of the ^{13}C NMR spectrum discontinuously vanishes; (3) Charge excitation gap (Δ_ρ) derived from the Arrhenius plot of ρ in the low-temperature CO state (Fig. 2(b)); (4) Spin excitation gap (Δ_{NMR}) derived from the Arrhenius plot of the nuclear relaxation rate ($1/T_1$) below T_{ss} (Fig. 2(b)).

T_{co} and T_{ss} essentially coincide with each other except for a small deference, which may be due to sample dependence or real internal pressures different run by run. Noticeably, Δ_ρ decreases more rapidly than T_{co} and T_{ss} by pressure and vanish for pressures above 8 kbar as indicated by the shaded gapless region ① in Fig. 2, suggesting the emergence of edge states in the CO state as theoretically predicted [5]. On the other hand, Δ_{NMR}, which corresponds to the (spin) gap inherent in the bulk phase, is robust against pressure in strong contrast with the behavior of Δ_ρ.

3.3 DF state

In the DF state, two contrasting renormalization behaviors in high and low energy ranges were observed. In a high-temperature regime above ca. 100 K, the local spin susceptibility probed by the Knight shift is gradually enhanced under decreasing pressure (Fig. 3(a)), which is consistent with the Stoner enhancement effect due to the screened Coulomb repulsion of short-range nature. On the other hand, in a low-temperature regime, the CO transition due to the inter-site Coulomb repulsion prevents the stabilization of Dirac cone at pressures below P_c; however, near-critical behaviors in the spin and charge degrees of freedom are observed in the DF state in the vicinity of P_c as indicated by region ② in the *P-T* phase diagram in Fig. 2(a). In region ②, first, the spin susceptibility (Fig. 3(a)) shows non-linear temperature dependence indicating the collapse of the linear dispersion of energy versus momentum;

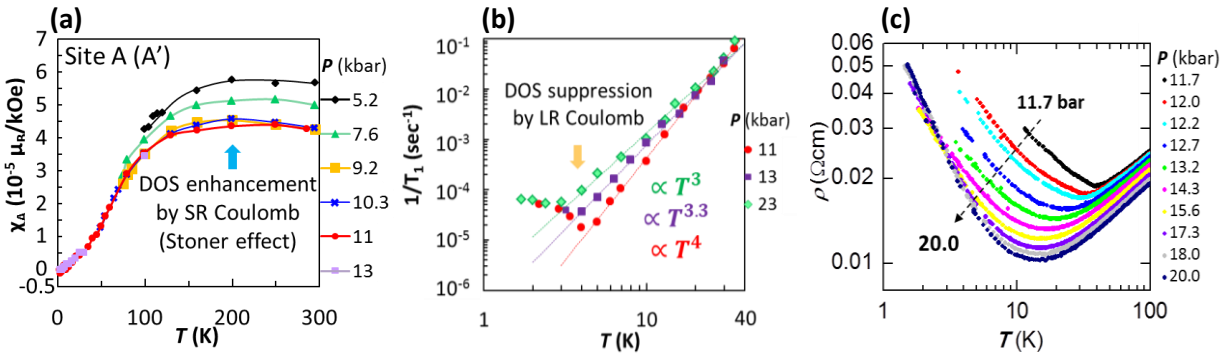

Fig. 3 (a) Spin susceptibility obtained from Knight Shift and (b) nuclear relaxation rate under different pressures (*P*=23 kbar: M. Hirata[6]). (c) Low temperature resistivity upturn in the critical region ② of DF state appears to be pushed toward lower temperatures by increasing pressure.

second, $1/T_1$ is gradually suppressed by decreasing pressure toward P_c (Fig. 3(b)); third, the low-temperature resistivity upturn (Fig. 3(c)) is progressively enhanced along with T_{min} on approaching P_c, suggesting the increase of the energy scale of the extra-coupling responsible for the anomalous non-metallic behavior.

These three features observed in region ② are considered to be manifestations of the effect of the long-range Coulomb interactions on the DF state and at least the latter two are demonstrated to be sensitive to the Coulomb interactions.

4. Conclusions

In this thesis work, we investigated the pressure evolution of the electronic state in the CO-DF system, α-I_3, through conducting electrical resistivity measurements and ^{13}C-NMR spectroscopy to probe the charge and spin behaviors, respectively. A *P*-*T* phase diagram is established, in which the CO-DF phase boundary for the ground state is clarified to be at approximately 11 kbar, appreciably different from the common beliefs of ～15 kbar. For the CO state, the existence of an edge state with a vanishing gap in the vicinity of the phase boundary is suggested by the extremely low energy charge excitations. For the DF state, we demonstrated that the spin susceptibility is enhanced at high temperatures while suppressed at low temperatures when the electron correlation strengthens by the pressure control. The contrasting behaviors at high and low temperatures are ascribable to the predominant roles of the short- and long-range Coulomb repulsions in the respective energy scales. Non-metallic behavior in resistivity at low temperatures is revealed to be intrinsic to the interacting DF system.

5. Reference

[1] H. Seo, J. Phys. Soc. Jap. **69**, 805 (2000).
[2] N. Tajima *et al.*, J. Phys. Soc. Jap. **69**, 543 (2000).
[3] S. Katayama *et al.*, J. Phys. Soc. Jap. **75**, 054705 (2006).
[4] J. Martin *et al.*, Nat. Phys. **4**, 144 (2008).
[5] Y. Omori *et al.*, JPS Conf. Proc. **1**, 012119 (2014).
[6] M. Hirata, Doctor's thesis, Dept. Appl. Phys., Univ. Tokyo (2012).